有机化学 DOI: 10.6023/cjoc202204032 研究论文
Chinese Journal of Organic Chemistry ARTICLE

水溶性萘酰亚胺类荧光探针对 Fe^{3+}和$Cr_2O_7^{2-}$的特异性检测

师春甜[a] 余 美[a] 吴爱斌*[,a,b] 罗江雄[c]
黎小军[a] 王宁晨[a] 舒文明[a,b] 余维初*[,a,b]
([a]长江大学化学与环境工程学院 湖北荆州 434023)
([b]长江大学非常规油气协同创新中心 湖北荆州 434023)
([c]湖南大学机械与运载工程学院 长沙 410082)

摘要 合成了一种能选择性识别 Fe^{3+}和 $Cr_2O_7^{2-}$ 的探针 *N*-(2-(2-(2-羟基乙氧基)乙基)-1,3-二氧基-2,3-二氢-1*H*-苯并[*de*]异喹啉-6-基)呋喃-2-甲酰胺(**1**), 这是首个基于萘酰亚胺检测 $Cr_2O_7^{2-}$ 的小分子探针. pH 滴定表明, 分子内电荷转移(intramolecular charge transfer, ICT)效应增强引起的光谱红移是酰胺负离子形成的结果, 还研究了探针 **1** 在 CH_3CN/*N*-2-羟乙基哌嗪-*N*′-2-乙磺酸(HEPES)缓冲溶液中对 Fe^{3+}和 $Cr_2O_7^{2-}$ 的选择性、浓度滴定、时间依赖性、猝灭常数、检测限和识别机理等. 研究表明, Fe^{3+}和 $Cr_2O_7^{2-}$ 通过内滤效应(IFE)快速猝灭探针 **1** 的荧光, 猝灭在 30 s 后恒定, 猝灭常数分别为 6.14×10^3 和 6.55×10^3 L•mol^{-1}; 探针 **1** 对 Fe^{3+}和 $Cr_2O_7^{2-}$ 的检测限分别为 1.62 和 1.56 μmol/L; 水样中 Fe^{3+}和 $Cr_2O_7^{2-}$ 的测定结果表明, 探针 **1** 可以作为一种在实际应用中的潜在检测工具.

关键词 荧光探针; $Cr_2O_7^{2-}$; Fe^{3+}; 萘酰亚胺; 内滤效应

A Water-Soluble Naphthalimide-Based Fluorescent Probe for Specific Sensing of Fe^{3+} and $Cr_2O_7^{2-}$

Shi, Chuntian[a] Yu, Mei[a] Wu, Aibin*[,a,b] Luo, Jiangxiong[c] Li, Xiaojun[a]
Wang, Ningchen[a] Shu, Wenming[a,b] Yu, Weichu*[,a,b]
([a] *School of Chemistry and Environmental Engineering, Yangtze University, Jingzhou, Hubei 434023*)
([b] *Unconventional Oil and Gas Collaborative Innovation Center, Yangtze University, Jingzhou, Hubei 434023*)
([c] *College of Mechanical and Vehicle Engineering, Hunan University, Changsha 410082*)

Abstract *N*-(2-(2-(2-Hydroxyethoxy)ethyl)-1,3-dioxo-2,3-dihydro-1*H*-benzo[*de*]isoquinolin-6-yl)furan-2-carboxamide (**1**) that can selectively recognize Fe^{3+} and $Cr_2O_7^{2-}$ was synthesized, which was the first small molecule probe based on naphthalimide to detect $Cr_2O_7^{2-}$. The pH titration showed that the spectral red shift caused by the enhancement of intramolecular charge transfer (ICT) effect was as a result of formation of amide anion. Besides, the selectivity, concentration titration, time dependence, quenching constant, detection limit and recognition mechanism of probe **1** to Fe^{3+} and $Cr_2O_7^{2-}$ were also studied in CH_3CN/*N*-2-hydroxyethylpiperazine-*N*′-2-ethanesulfonic acid (HEPES) buffer solution. The results showed that Fe^{3+} and $Cr_2O_7^{2-}$ could rapidly quenched the fluorescence of probe **1** through the inner filter effect. The quenching effects remained constant after 30 s, and the quenching constants were 6.14×10^3 and 6.55×10^3 L•mol^{-1}, respectively. The detection limits of probe **1** for Fe^{3+} and $Cr_2O_7^{2-}$ were 1.62 and 1.56 μmol/L, respectively. The determination of Fe^{3+} and $Cr_2O_7^{2-}$ in water samples made it clear that probe **1** could be used as a potential detection tool in practical application.

Keywords fluorescent probe; $Cr_2O_7^{2-}$; Fe^{3+}; naphthalimide; inner filter effect

1 Introduction

With the rapid development of modern industry and agriculture, more and more toxic heavy metal ions, inorganic anions, small organic molecules, antibiotics and pesticides enter the environment and become the main pollution

* Corresponding authors. E-mail: abwu@yangtzeu.edu.cn; yuweichu@126.com
Received April 13, 2022; revised June 2, 2022; published online July 20, 2022.
Project supported by the National Science and Technology Major Project of China (No. 2017ZX05049-003-007) and the National Natural Science Foundation of China (No. 21801022).
国家科技重大专项基金(No. 2017ZX05049-003-007)及国家自然科学基金(No. 21801022)资助项目.

source in water.[1-2] Therefore, it inevitably poses a serious threat to human life, health and living environment.[3-4] Fe^{3+} is an essential trace element in organisms.[5-8] The human body requires about 30 mg per day to maintain a variety of life activities,[9] such as protein synthesis, osmotic pressure regulation, pH balance stability, hemoglobin formation, oxygen metabolism, cytochrome, enzyme catalysis, photocatalysis and electron transfer in DNA and RNA synthesis.[10-17] However, insufficient or excessive Fe^{3+} content can lead to many health problems.[12,14-15] Excessive Fe^{3+} ion in the body may lead to the risk of osteoporosis, hemochromatosis, diabetes, depression, hepatitis, organ failure, respiratory problems, convulsions, cardiac arrest, ucleic acid and protein damage, gastrointestinal diseases and other diseases.[5-6,8,11,13,18-19] At the same time, insufficient Fe^{3+} ion in the human body will induce Parkinson's disease, Huntington's disease, Alzheimer's disease, anemia, insomnia and hair loss.[1,9,17,20] It is well known that chromium is a heavy metal element, and its two oxidation states (Cr^{3+} and Cr^{6+}) dominate in water and soil.[21,22] Although Cr^{3+} is a necessary trace ion for mammals,[21] excessive Cr^{3+} will bind to DNA and destroy cell structure.[23] Cr^{6+} is a toxic ion, and even low concentration of Cr^{6+} can pose a threat to life and health,[24-25] such as respiratory diseases, gastrointestinal diseases, skin damage, kidney diseases, central nervous system diseases, tumors, cancers, malformations and gene mutations.[24-28] As an anionic salt of Cr^{6+}, $Cr_2O_7^{2-}$ also has high toxicity, carcinogenicity, teratogenicity and bioaccumulation.[29-32] Long term exposure to the environment with $Cr_2O_7^{2-}$ anion may lead to some adverse health effects, including allergic reaction, renal failure, rhinitis, gene mutation, cancer, *etc*.[3,28,33-35] $Cr_2O_7^{2-}$ is not only identified as "A" carcinogen by the world health organization (WHO),[19,25,34] but also listed as a priority pollutant by the U. S. A. Environmental Protection Agency (EPA).[31,36] Therefore, it is of great significance to determine the contents of Fe^{3+} and $Cr_2O_7^{2-}$ ions in the environment and organisms for life health, environmental safety and medical diagnosis and treatment.

To date, various analytical methods have been used to detect metal ions and anions, including chromatography, mass spectrometry, electrochemical atomic absorption/emission spectrometry, graphite flame atomic absorption spectrometry, voltammetry, solid phase microextraction, high performance liquid chromatography, inductively coupled plasma atomic emission spectrometry, plasma resonance rayleigh scattering spectroscopy, Raman spectroscopy, spectrophotometry and ion mobility spectroscopy.[3,7,15,22,32,37-39] However, most of these technologies have high cost, low sensitivity, long time-consuming, complex preprocessing and need skilled operators.[8,17,26,35] In contrast, fluorescent probe detection has the characteristics of high selectivity, high sensitivity, low cost, rapid response, visualization and biological imaging, which can make up for the shortcomings of traditional analytical methods.[11,15-16,24,37] At present, there are many reports on fluorescence sensing for the detection of Fe^{3+}, including organic small molecules,[4-6,11-12,16,18,20,26] metal organic frameworks [2,7-8,10,38,40-42], quantum dots and so on.[9,13-15,39,43] However, when considering the practical application ability of the probe in selectivity, sensitivity, competitiveness and applicable conditions, researchers believe that there is still a need for development and progress for Fe^{3+} fluorescent sensors.[6,11,15,39] Compared with the fluorescence sensor of Fe^{3+}, there are fewer reports on the fluorescence sensor of $Cr_2O_7^{2-}$, and most of them are based on metal-organic framework (MOFs) sensors, such as Zn-MOFs,[1,31-32,35-36,44] Cd-MOFs,[25,33-34,45] Co-MOFs,[2] In-MOFs,[46] Eu-MOFs,[47] Mn-MOFs,[48] Zr-MOFs[28] and Pb-MOFs.[48] Although the preparation process of MOFs sensors is relatively simple, it is not enough safe, convenient and quick, because the preparation or detection process may cause metal ions such as Zn^{2+}, Co^{2+}, Cd^{2+}, Eu^{2+}, Mn^{2+}, Pb^{2+} to enter the environment, and most of the detection processes require ultrasonic treatment or room temperature storage for a certain time.[2,27,34-35,44-48] Thus, it is very promising and necessary to develop fluorescent probes for Fe^{3+} and $Cr_2O_7^{2-}$ ions with convenient detection, sensitive response, safe use and strong practicability.

1,8-Naphthalimide is the photosensitive part of photochemical sensor. It not only has large rigid plane and conjugated π system, but also has the characteristics of bright color and fluorescence, good light stability, high fluorescence quantum yield and easy modification.[49-51] Therefore, naphthalimides are widely used as fluorophores in probes structure design. In this paper, we reported naphthalimide-based probe **1** with selectivity, sensitivity and rapid response for Fe^{3+} and $Cr_2O_7^{2-}$ ions, and realized its practical application for the determination of Fe^{3+} and $Cr_2O_7^{2-}$ in drinking water. Furthermore, probe **1** is the first organic small molecule probe based on naphthalimide for detecting $Cr_2O_7^{2-}$, which has higher water solubility, sensitivity, convenience and practicability than the reported probes. Probe **1** was prepared according to the synthetic route shown in Scheme 1 and its structure was identified by NMR and MS analysis.

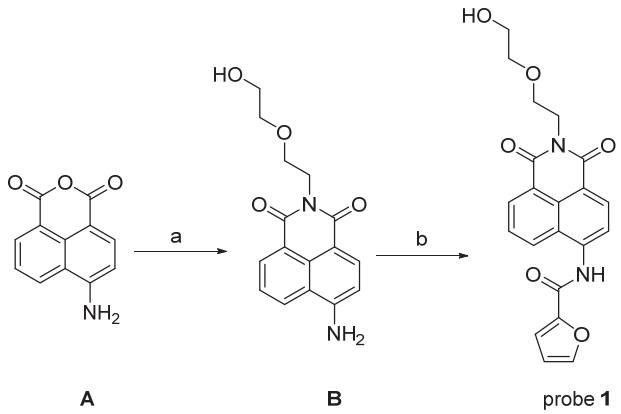

Reagents and conditions: (a) 2-(2-aminoethoxy)ethanol, DMF, 150 ℃; (b) furoyl chloride, Et_3N, CH_3CN, 90 ℃.

Scheme 1 Synthesis of probe **1**

2 Results and discussion

The test medium plays a major role in the fluorescence properties of the probe. In this study, common solvents that can be miscible with water will be selected as the test medium of probe **1**. The results showed that probe **1** had the most sensitive fluorescence emission in CH_3CN, and CH_3CN was selected as the experimental medium to further explore the fluorescence performance of probe **1**.

2.1 Study on pH interference of probe 1

To eliminate the interference caused by pH in the process of identifying analytes, the fluorescence titration experiment of probe **1** about pH was carried out in the environment of CH_3CN/H_2O (V∶V=1∶9) (Figure 1, a). The curves relationship between fluorescence emission intensity of probe **1** at 463 nm and pH value was established (Figure 1, b). The results showed that fluorescence intensity of probe **1** remained almost constant when the pH range was 1.67～9.66. When pH≥10.91, the fluorescence intensity of probe **1** decreased dramatically or disappeared gradually at 463 nm. When pH≥12.87, the emission peak of probe **1** clearly showed obvious red-shift to 568 nm.

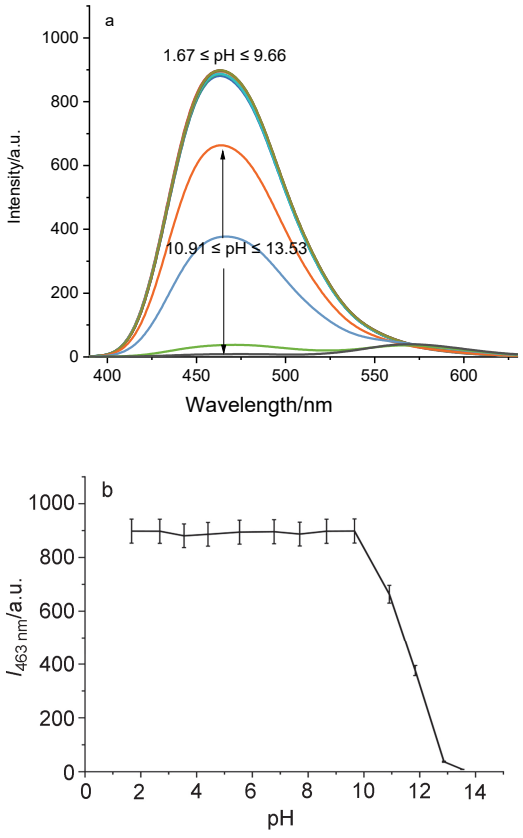

Figure 1 (a) Fluorescence spectra of probe **1** (10 μmol/L, CH_3CN/H_2O, V∶V=1∶9) under different pH and (b) curves between fluorescence intensity of probe **1** at 463 nm and different pH values

To reveal the reason of the fluorescence change of probe **1** caused by the change of pH value, the UV-Vis spectra of probe **1** were scanned about pH titration. The UV-Vis absorption spectra and fluorescence emission spectra of probe **1** showed a high agreement in the process of pH titration. The ultraviolet absorption peaks of probe **1** were assigned, in which the absorption peak at 292 nm was due to the n-π* transition of furan group and the absorption peak at 363 nm was due to the n-π* transition of C=O double bond in amide group. Moreover, since the amide group could form amide negative ion under alkaline conditions, which may lead to enhancement of intramolecular charge transfer (ICT) effect and spectral red-shift caused by the enhancement of power supply capacity at position 4 of naphthalimide fluorophore. Therefore, the fluorescence change mechanism of probe **1** under strong alkali conditions was reasonably and accurately provided (Scheme 2).

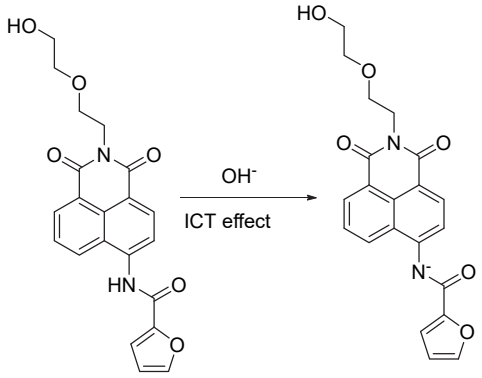

Scheme 2 Response mechanism of spectra of probe **1** under strong basic conditions

2.2 Recognition properties and mechanism of probe 1 to Fe^{3+}

Based on the excellent fluorescence properties of probe **1**, its cation recognition performance was further explored (Figure 2). Under 300 nm excitation wavelength, the cations were added to the CH_3CN/*N*-2-hydroxyethylpiperazine-*N*′-2-ethanesulfonic acid (HEPES) buffer solution (V∶V=

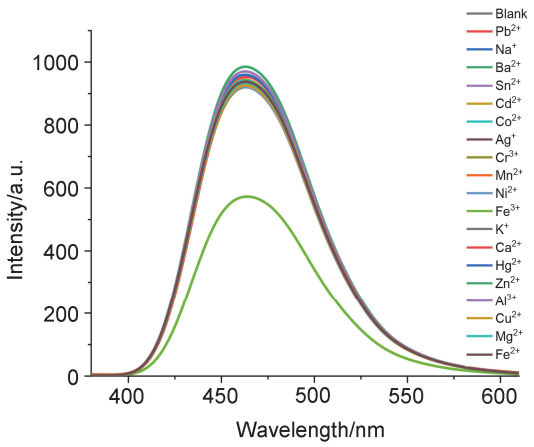

Figure 2 Fluorescence spectra of probe **1** in CH_3CN/HEPES (V∶V=1∶9, 10 mmol/L, pH=7.4) buffer solution upon addition of Pb^{2+}, Na^+, Ba^{2+}, Sn^{2+}, Cd^{2+}, Co^{2+}, Ag^+, Cr^{3+}, Mn^{2+}, Ni^{2+}, Fe^{3+}, K^+, Ca^{2+}, Hg^{2+}, Zn^{2+}, Al^{3+}, Cu^{2+}, Mg^{2+} and Fe^{2+} ions

1∶9, 10 mmol/L, pH=7.4) of probe **1** with a concentration of 10 μmol/L, respectively. Compared with the fluorescence quenching caused by Fe^{3+}, the fluorescence changes caused by the ions involved in the test could be ignored. Obviously, probe **1** could be used as an effective fluorescent probe to recognize Fe^{3+}.

Fe^{3+} ion was added to the CH_3CN/HEPES (V∶V=1∶9, 10 mmol/L, pH=7.4) buffer solution of probe **1** with a concentration of 10 μmol/L to establish the curvilinear relationship between Fe^{3+} concentration and fluorescence intensity of probe **1** (Figures 3a and 3b). It could be seen that with the increase of Fe^{3+} ion concentration, the fluorescence intensity of probe **1** at 463 nm decreased gradually, and the curve between the fluorescence intensity and Fe^{3+} concentration deviated from linearity gradually. Therefore, the appropriate Fe^{3+} concentration was selected to establish a linear relationship with the fluorescence intensity of probe **1** at 463 nm. The linear relationship was $y=918.80-4.50x$ ($R^2=0.997$). Therefore, probe **1** could be used as a potential fluorescent probe to accurately detect Fe^{3+} with a concentration of 0～50 μmol/L.

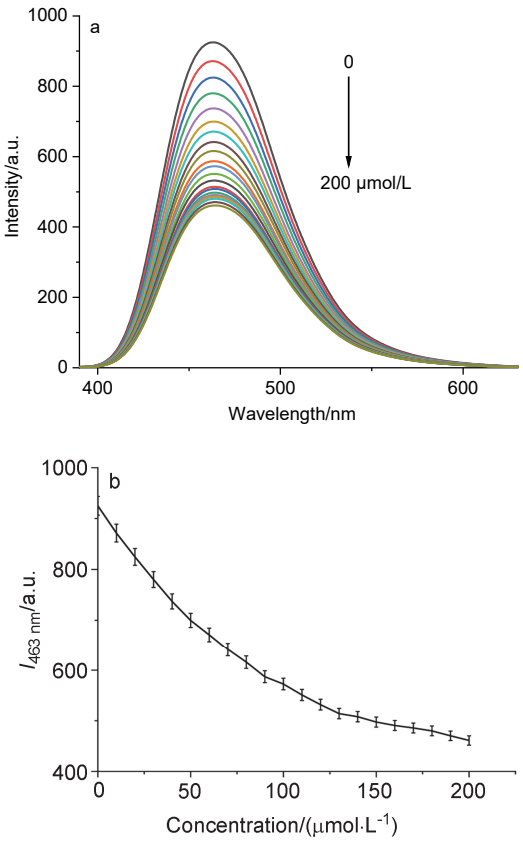

Figure 3 (a) Fluorescence titration spectra of probe **1** in CH_3CN/HEPES (V∶V=1∶9, 10 mmol/L, pH=7.4) buffer solution upon addition of Fe^{3+} and (b) curves between fluorescence intensity of probe **1** at 463 nm and different Fe^{3+} concentration

For evaluating the quenching efficiency caused by Fe^{3+}, the quenching constant was calculated by the Stern-Volmer (SV) equation: $I_0/I=1+K_{sv}[M]$ (where I_0 and I are the emission intensity of probe **1** in the absence and presence of Fe^{3+}, K_{sv} is the quenching constant and [M] is the Fe^{3+} concentration). The result was $K_{sv}=6.14\times10^3$ L•mol^{-1}. In addition, the formula $D=3\delta/K$ (where D is the detection limit of Fe^{3+} recognized by probe **1**, δ is the standard deviation of fluorescence intensity of blank sample scanned for 15 times, and K is the slope value of the linear relationship between fluorescence intensity and Fe^{3+} concentration) was used to calculate the limit concentration of probe **1** in response to Fe^{3+}. The results were $\delta=2.59$, $K=4.80$, $D=1.62$ μmol/L. The detection limit was lower than the maximum allowable concentration of Fe^{3+} in drinking water specified by China's drinking water standard (GB 5749-2006) and the U. S. A. EPA, which was 5.36 μmol/L.

The time-dependent spectra of probe **1** in response to Fe^{3+} were measured, and the curve between the fluorescence intensity of probe **1** at 463 nm and the addition time of Fe^{3+} were also established. The results showed that the fluorescence of probe **1** could be quenched rapidly by Fe^{3+}, stabilized within 30 s and remained stable at least 60 min.

The UV-Vis spectra of probe **1** were recorded with the addition of Fe^{3+}. It was found that the absorption peaks increased and slightly blue-shifted, and a wide absorption band appeared in the range of 400～550 nm. These phenomena were inconsistent with the fluorescence emission spectrum of probe **1** added with Fe^{3+} ion. Further, we scanned the UV-Vis spectra of probe **1** and Fe^{3+}, and the fluorescence spectrum probe **1** (Figure 4). Obviously, Fe^{3+} ion has ultraviolet absorption, and the absorption band overlaps with the absorption band and emission band of the probe **1**. Based on a series of fluorescence and UV-Vis spectral behaviors of Fe^{3+} recognized by probe **1**, these indicate that the recognition mechanism is not due to the structural collapse of probe **1** and the complexation between probe **1** and Fe^{3+}, which is due to the inner filter effect (IFE) mechanism. These spectral phenomena had been reported previously in literature.[1,31,33,35,40] Researchers believe that fluorescence quenching is due to the energy competition caused by the absorption overlap between the probe and the analyte, and the deviation from linearity in the relationship

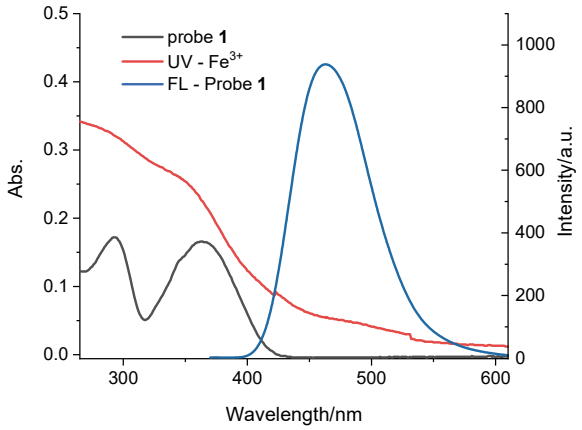

Figure 4 Absorption spectra of probe **1** and Fe^{3+} and the fluorescence spectrum probe **1** in CH_3CN/HEPES (V∶V=1∶9, 10 mmol/L, pH=7.4) buffer solution.

between fluorescence intensity and analyte concentration is due to the energy transfer caused by the emission of the probe overlap the absorption of the analyte.

2.3 Recognition properties and mechanism of probe **1** to $Cr_2O_7^{2-}$

Besides, its anion recognition performance was explored (Figure 5). Obviously, $Cr_2O_7^{2-}$ could quench the fluorescence of probe **1**.

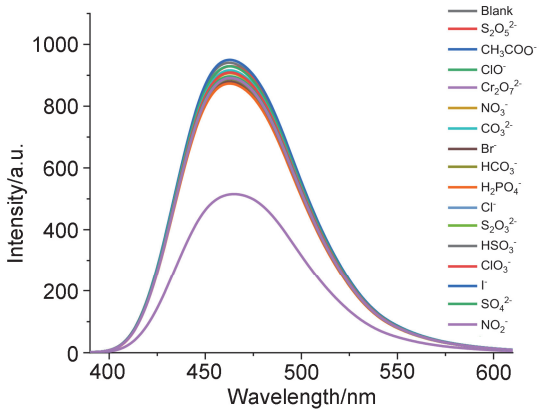

Figure 5 Fluorescence emission spectra of probe **1** in CH_3CN/HEPES (V∶V=1∶9, 10 mmol/L, pH=7.4) buffer solution upon addition of $Cr_2O_7^{2-}$, $S_2O_5^{2-}$, CH_3COO^-, ClO^-, NO_3^-, CO_3^{2-}, Br^-, HCO_3^-, $H_2PO_4^-$, Cl^-, $S_2O_3^{2-}$, HSO_3^-, ClO_3^-, I^-, SO_4^{2-} and NO_2^- ions

The $Cr_2O_7^{2-}$ ion was added to the CH_3CN/HEPES (V∶V=1∶9, 10 mmol/L, pH=7.4) buffer solution of probe **1** to obtain the fluorescence titration spectra and the change trend was established (Figures 6a and 6b). It could be seen that the fluorescence intensity of probe **1** at 463 nm decreases gradually with the increase of $Cr_2O_7^{2-}$, and the curves between the fluorescence intensity of probe **1** and the concentration of $Cr_2O_7^{2-}$ deviated from linearity gradually. Therefore, the $Cr_2O_7^{2-}$ of 0～50 μmol/L were selected to establish a linear relationship with the fluorescence intensity of probe **1** at 463 nm. Clearly, probe **1** could be used as a fluorescent probe to accurately detect $Cr_2O_7^{2-}$ ion with a concentration of 0～50 μmol/L, and the linear relationship was y=929.18−4.97x (R^2=0.996).

The quenching constant was 6.55×10^3 L•mol^{-1}, and the detection limit was 1.56 μmol/L. The detection limit was less than the maximum allowable concentration of $Cr_2O_7^{2-}$ in water by the U. S. A. EPA (1.92 μmol/L). Similarly, the time-dependent spectra of probe **1** in response to $Cr_2O_7^{2-}$ were measured. The results showed that the fluorescence of probe **1** could be quenched rapidly by $Cr_2O_7^{2-}$, and stabilized within 30 s and remained stable at least 60 min.

By studying the absorption spectral response of the probe **1** to anions and the spectral overlap between the probe **1** and $Cr_2O_7^{2-}$ (Figure 7), it was proved that the response mechanism of probe **1** to $Cr_2O_7^{2-}$ was the same as that of Fe^{3+}, which was the IFE. Further, similar spectral behaviors had been recorded in previously reported literatures.[25,27,32,35,45-46,52-53]

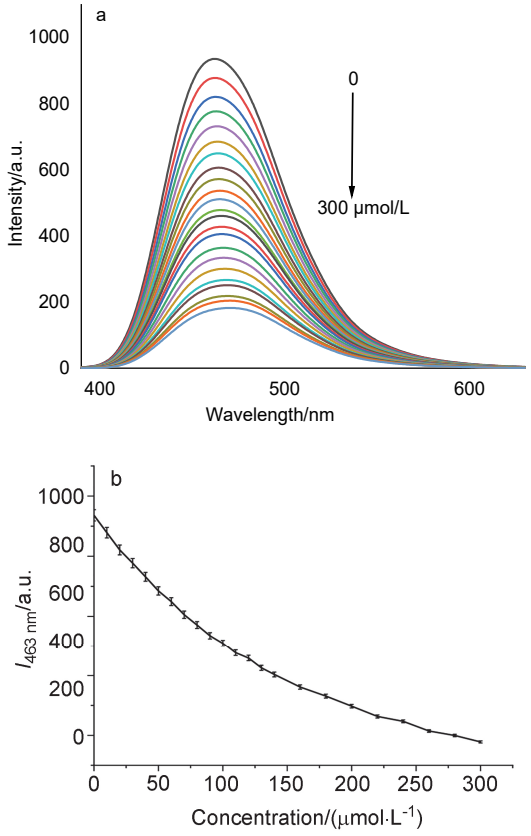

Figure 6 (a) Fluorescence titration spectra of probe **1** in CH_3CN/HEPES (V∶V=1∶9, 10 mmol/L, pH=7.4) buffer solution upon addition of $Cr_2O_7^{2-}$ and (b) curves between fluorescence intensity of probe **1** at 463 nm and different $Cr_2O_7^{2-}$ concentration

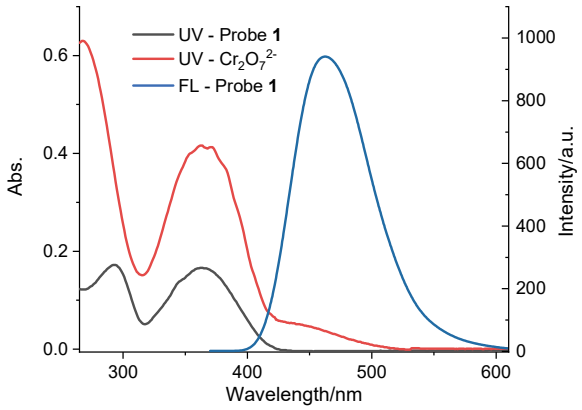

Figure 7 Absorption spectra of probe **1** and $Cr_2O_7^{2-}$, and the fluorescence spectrum of probe **1** in CH_3CN/HEPES (V∶V=1∶9, 10 mmol/L, pH=7.4) buffer solution

2.4 Differentiation of Fe^{3+} and $Cr_2O_7^{2-}$ by probe **1**

In order to distinguish Fe^{3+} from $Cr_2O_7^{2-}$, EDTA was added as chelating agent or auxiliary agent of Fe^{3+} to shield the fluorescence quenching caused by Fe^{3+} when the probe **1** was detecting $Cr_2O_7^{2-}$ (Figure 8). It was obvious that EDTA hardly affected the fluorescence of probe **1** and the fluorescence of probe **1** recognizing Fe^{3+} or $Cr_2O_7^{2-}$.

Therefore, EDTA can not be used as an auxiliary or chelating agent for probe **1** to distinguish Fe^{3+} and $Cr_2O_7^{2-}$, and EDTA can not realize the reversible application of probe **1**.

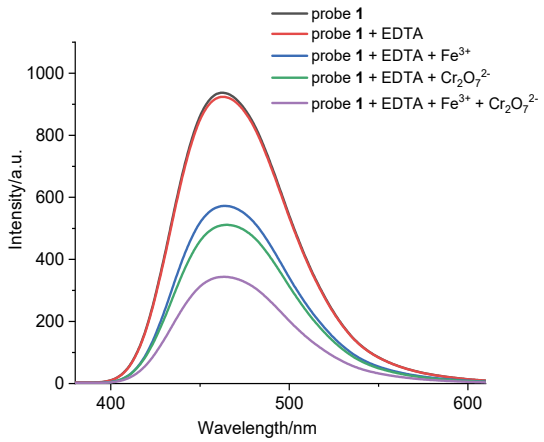

Figure 8 Discrimination of Fe^{3+} and $Cr_2O_7^{2-}$ and the reversibility of probe **1** assisted by EDTA

2.5 Water sample detection of Fe^{3+} and $Cr_2O_7^{2-}$ by probe **1**

In order to assess the practicability of probe **1**, the detection was carried out in water samples (Table 1). Obviously, the found values of Fe^{3+} and $Cr_2O_7^{2-}$ in water samples were very close to the added value of Fe^{3+} and $Cr_2O_7^{2-}$, respectively. The values of relative standard deviation (RSD) were less than 3.30% and 2.31%. This clearly indicated that probe **1** could be used as a potential tool in practical application.

Table 1 Determination of Fe^{3+} and $Cr_2O_7^{2-}$ in water samples (n=5).

Tested ion	Ion added/ (μmol•L^{-1})	Ion found/ (μmol•L^{-1})	Recovery/%	RSD/%
Fe^{3+}	2.00	2.13	106.50	3.30
	5.00	5.20	104.00	1.01
	10.00	10.34	103.40	1.97
$Cr_2O_7^{2-}$	2.00	1.98	99.00	2.31
	5.00	5.01	100.20	1.94
	10.00	9.99	99.90	0.99

3 Conclusions

In conclusion, a water-soluble probe that can recognize Fe^{3+} and $Cr_2O_7^{2-}$ based on the inner filter effect has been developed. When the pH value was high, due to the formation of amide anion strengthening the ICT effect, the spectra of probe **1** were red-shifted. In CH_3CN/HEPES (V∶V=1∶9, 10 mmol/L, pH=7.4) buffer solution, probe **1** could be rapidly quenched by Fe^{3+} and $Cr_2O_7^{2-}$, respectively, and the quenching constants were 6.14×10^3 and 6.55×10^3 L•mol^{-1}. The detection limits of probe **1** for Fe^{3+} and $Cr_2O_7^{2-}$ were 1.62 and 1.56 μmol/L, respectively, which were lower than the maximum allowable concentration values of Fe^{3+} and $Cr_2O_7^{2-}$ in drinking water specified by the EPA. Moreover, the result of practical application in water samples indicated that the probe could be used as a potential tool for detecting Fe^{3+} and $Cr_2O_7^{2-}$. This work provided a new method with selectivity, sensitivity, convenient detection and potential practicability for detecting Fe^{3+} and $Cr_2O_7^{2-}$.

4 Experimental section

4.1 General

All the analytical grade reagents and solvents were purchased from commercial sources and used as received without further purification. An aqueous solution with a concentration of 0.01 mol/L was prepared from chlorides or nitrates of metal ions (Pb^{2+}, Na^+, Ba^{2+}, Sn^{2+}, Cd^{2+}, Co^{2+}, Ag^+, Cr^{3+}, Mn^{2+}, Ni^{2+}, Fe^{3+}, K^+, Ca^{2+}, Hg^{2+}, Zn^{2+}, Al^{3+}, Cu^{2+}, Mg^{2+} and Fe^{2+}). An anionic aqueous solution with a concentration of 0.01 mol/L ($Cr_2O_7^{2-}$, $S_2O_5^{2-}$, CH_3COO^-, ClO^-, NO_3^-, CO_3^{2-}, Br^-, HCO_3^-, $H_2PO_4^-$, Cl^-, $S_2O_3^{2-}$, HSO_3^-, ClO_3^-, I^-, SO_4^{2-} and NO_2^-) was prepared from sodium or potassium salts. The concentration of ClO^- was determined at 292 nm (ε=365 L•mol^{-1}•cm^{-1}).

NMR spectra were determined on a Bruker Avance 400 MHz instrument. Chemical shifts of NMR were given relative to tetramethyl silane (TMS) and referenced to the solvent signal. Melting points were measured on an X-4 digital melting-point apparatus. HRMS (ESI) was measured on an Agilent 1100 LC-MSD-Trap-VL system. Elemental analyses were performed by a CARLOERBA-1106 microelemental analyzer. UV-Vis absorption spectra were conducted on a PerkinElmer Lambda 650 spectrophotometer. Luminescent spectra of the obtained samples were recorded on a PerkinElmer LS55 spectrophotometer.

4.2 Synthesis

The preparation of compound **A** referred to the reported literature.[54-55] Acenaphthene was used as raw material, and **A** was obtained through nitration, oxidation and reduction reactions. Orange solid, 90.1% yield. m.p. 284.1～285.2 ℃; ^{1}H NMR (400 MHz, DMSO-d_6) δ: 8.92～8.00 (m, 3H), 7.74 (d, J=70.3 Hz, 3H), 6.87 (s, 1H); ^{13}C NMR (100 MHz, DMSO-d_6) δ: 162.50, 160.82, 154.40, 136.39, 133.51, 133.07, 131.18, 124.88 119.78, 118.77, 109.20, 102.71; MS (ESI) m/z: 212.0 [M−H]$^-$; Anal. calcd for $C_{12}H_7NO_3$: C 67.61, H 3.31, N 6.57, O 22.51; found C 67.60, H 3.31, N 6.58, O 22.52.

Compound **A** (400 mg, 1.88 mmol) and *N*,*N*′-dimethylformamide (DMF) (2 mL) were taken to reflux at 150 ℃, and diethylene glycol amine (250 μL, 2.50 mmol) was added dropwise. After thin-layer chromatography (TLC) monitoring showed that the reaction was completed, the solution was cooled to room temperature and water was added to separate out the product. The residue was collected by suction filtration, and washed with water and absolute ethanol to obtain 581.3 mg of compound **B**. Orange solid, 89.5% yield. m.p.＞300 ℃; ^{1}H NMR (400 MHz, DMSO-d_6) δ: 8.67～8.54 (m, 1H), 8.47～8.34 (m, 1H), 8.19 (dd,

J=8.3, 2.6 Hz, 1H), 7.70～7.57 (m, 1H), 7.45 (s, 2H), 6.89～6.75 (m, 1H), 4.57 (s, 1H), 4.20 (d, J=6.3 Hz, 2H), 3.62 (t, J=6.3 Hz, 2H), 3.47 (s, 4H); ^{13}C NMR (100 MHz, DMSO-d_6) δ: 164.30, 163.36, 153.24, 134.48, 131.53, 130.20, 129.83, 124.44, 122.15, 119.82, 108.65, 107.88, 72.55, 67.57, 60.66, 38.79; MS (ESI) m/z: 299.2 $[M-H]^-$; Anal. calcd for $C_{16}H_{16}N_2O_4$: C 63.99, H 5.37, N 9.33, O 21.31; found C 63.98, H 5.35, N 9.37, O 21.32.

Compound **B** (102.2 mg, 0.34 mmol) and acetonitrile (2 mL) were taken to reflux at 110 ℃, and furoyl chloride (75 μL) and triethylamine (85 μL) were added dropwise. After TLC monitoring showed that the reaction was completed, column separation was carried out with CH_2Cl_2/CH_3OH (V∶V=50∶1) to obtain 98.20 mg of probe **1**. Bright yellow solid, 73.3% yield. m.p.＞300 ℃; ^{1}H NMR (400 MHz, DMSO-d_6) δ: 10.78 (s, 1H), 8.57～8.48 (m, 3H), 8.09 (d, J=8.0 Hz, 1H), 8.04 (dd, J=1.7, 0.7 Hz, 1H), 7.88 (dd, J=8.5, 7.3 Hz, 1H), 7.53 (dd, J=3.5, 0.7 Hz, 1H), 6.79 (dd, J=3.5, 1.7 Hz, 1H), 4.57 (s, 1H), 4.26 (t, J=6.5 Hz, 2H), 3.67 (t, J=6.5 Hz, 2H), 3.48 (s, 4H); ^{13}C NMR (100 MHz, DMSO-d_6) δ: 163.95, 163.47, 157.43, 147.45, 146.87, 140.08, 131.57, 131.57, 130.73, 128.78, 127.12, 126.47, 123.24, 122.67, 119.47, 116.33, 112.83, 72.59, 67.39, 60.66, 39.24; HRMS (ESI) calcd for $C_{21}H_{18}N_2O_6$ $[M+H]^+$ 395.1243, found 395.1230. Anal. calcd for $C_{21}H_{19}N_2O_6$: C 63.96, H 4.60, N 7.10, O 24.34; found C 63.97, H 4.64, N 7.06, O 24.36.

4.3 Fluorescence response experiments

4.3.1 Solvent selection

Since the probe has different luminescence properties in different solvents, common water-soluble organic solvents were selected. The dimethyl sulfoxide (DMSO) solution of probe **1** was taken with a concentration of 1 mmol/L and the solutions of CH_3CN, CH_3OH, CH_3CH_2OH, DMSO, DMF, and H_2O were prepared with concentration of 10 μmol/L. Then, 3 mL of probe solutions in different solvents were taken at an excitation wavelength of 300 nm, and the fluorescence emission spectra of probes in different solvents were collected.

4.3.2 pH response

In order to study the effect of different pH test environments on the fluorescence emission spectra of the probe, the CH_3CN/H_2O solutions of probe **1** was prepared with a concentration of 10 μmol/L and different pH values were adjusted. The fluorescence emission spectra of probe **1** in different pH test environments were measured at an excitation wavelength of 300 nm.

4.3.3 Ion response

Because probe **1** has excellent fluorescence properties, the fluorescence emission spectra of probe **1** with concentration of 10 μmol/L in CH_3CN/HEPES (V∶V=1∶9, 10 mmol/L, pH＝7.4) buffer solution and excitation wavelength of 300 nm was studied. To evaluate the selectivity and utility of the response of probe **1** to ions, selectivity experiments as well as fluorescence titration experiments, detection limit calculations, and response time measurements for the selectively responsive ions were performed. In addition, according to the UV-Vis absorption spectra and fluorescence emission spectra of the responsive ions of probe **1**, the mechanism of the selective response of ions of probe **1** was rationally explained.

4.4 Tap water detection with probe

Water samples were collected from the taps of the School of Chemical and Environmental Engineering, Yangtze University, and the same concentrations of ions were added to 5 natural water samples. The RSD of 5 samples and the recovery of spiked samples during analysis were calculated based on the fluorescence response of probe **1** to evaluate the practicability and accuracy of the probe in practical applications.

Supporting Information Performance comparison between probe **1** and reported probes, fluorescence emission spectra of probe **1** in different solvents, UV-Vis absorption spectra of probe **1** under different pH, linear relationship between fluorescence intensity of probe **1** at 463 nm and concentration of Fe^{3+}, the variation curve of fluorescence intensity of probe **1** at 463 nm with Fe^{3+} ion addition time, UV-Vis absorption spectra of probe **1** upon addition of cations, linear relationship between fluorescence intensity of probe **1** at 463 nm and concentration of $Cr_2O_7^{2-}$ ion, the variation curve of fluorescence intensity of probe **1** at 463 nm with $Cr_2O_7^{2-}$ ion addition time, UV-Vis absorption spectra of probe **1** upon addition of anions, and the ^{1}H NMR, ^{13}C NMR and ESI-MS analysis of intermediate and probe **1**. The Supporting Information is available free of charge via the Internet at http://sioc-journal.cn.

References

[1] Ma, Z. L.; Wang, M. C.; Tian, L.; Cheng, L. *Inorg. Chim. Acta* **2021**, *526*, 120513.

[2] Zhang, Z.; Sun, H. X.; Li, S. F.; Wang, R. D.; Du, L.; Xie, M. J.; Zhou, J.; Zhao, Q. H. *J. Inorg. Organomet. Polym.* **2021**, *31*, 2063.

[3] Ma, X.; Han, L.; Zhang, X.; Hao, Z.; Yang, W.; Zhang, Y.; Wang, L. *Chin. J. Org. Chem.* **2020**, *40*, 2938 (in Chinese).
(马学林, 韩利民, 张骁勇, 郝占忠, 杨威, 张玉恒, 王丽, 有机化学, **2020**, *40*, 2938.)

[4] Hu, J. P.; Yang, H. H.; Lin, Q.; Yao, H.; Zhang, Y. M.; Wei, T. B.; Qu, W. J. *Photochem. Photobiol. Sci.* **2020**, *19*, 1690.

[5] Zhang, Y. P.; Li, X. F.; Yang, Y. S.; Wang, J. L.; Zhao, Y. C.; Xue, J. J. *J. Fluoresc.* **2021**, *31*, 29.

[6] Dwivedi, S. K.; Ali, R.; Singh, M.; Gupta, T.; Kar, A. K.; Prakash, V.; Sadasivam, A.; Patnaik, S.; Misra, A. *J. Photochem. Photobiol., A* **2020**, *403*, 112854.

[7] Song, S.; Hu, J.; Li, M.; Gong, X.; Dong, C.; Shuang, S. *Mater. Sci. Eng., C* **2021**, *118*, 111478.

[8] Fajal, S.; Samanta, P.; Dutta, S.; Ghosh, S. K. *Inorg. Chim. Acta* **2020**, *502*, 119359.

[9] Dong, Y.; Zhang, Y.; Zhi, S.; Yang, X.; Yao, C. *ChemistrySelect* **2021**, *6*, 123.

[10] Zhang, T.; Salah, A.; Chang, S.; Zhang, Z.; Wang, G. *Tetrahedron* **2021**, *96*, 132405.

[11] Liu, Y.; Zhao, C.; Zhao, X.; Liu, H.; Wang, Y.; Du, Y.; Wei, D. *J. Environ. Sci.* **2020**, *90*, 180.

[12] Hossain, S. M.; Dam, G. K.; Mishra, S.; Singh, A. K. *New J. Chem.*

2020, *44*, 15186.
[13] Kalaiyarasan, G.; Joseph, J.; Kumar, P. *ACS Omega* **2020**, *5*, 22278.
[14] Deng, H.; Tian, C.; Gao, Z.; Chen, S.-W.; Li, Y.; Zhang, Q.; Yu, R.; Wang, J. *Analyst* **2020**, *145*, 4931.
[15] Huang, Z.; Gao, Y.; Huang, Z.; Chen, D.; Sun, J.; Zhou, L. *Microchem. J.* **2021**, *170*, 106656.
[16] Huang, J.; Yan, Z.; Qiu, P.; Mo, Y.; Cao, Q.; Li, Q.; Huo, L.; Zhao, L. *Molecules* **2021**, *26*, 2115.
[17] Shellaiah, M.; Thirumalaivasan, N.; Aazaad, B.; Awasthi, K.; Sun, K. W.; Wu, S. P.; Lin, M. C.; Ohta, N. *Spectrochim. Acta*, *Part A* **2020**, *242*, 118757.
[18] Nootem, J.; Sattayanon, C.; Daengngern, R.; Kamkaew, A.; Wattanathana, W.; Wannapaiboon, S.; Rashatasakhon, P.; Chansaenpak, K. *Chemosensors* **2021**, *9*, 165.
[19] Sun, J.; Guo, P.; Liu, M.; Li, H. *J. Mater. Chem. C* **2019**, *7*, 8992.
[20] Sayed, A.; Othman, I. M. M.; Hamam, M.; Gomaa, H.; Gadallah, M. I.; Mostfa, M. A.; Ali, H. R. H.; Emran, M. Y.; Abdel-Hakim, M.; Mahross, M. H. *J. Mol. Struct.* **2021**, *1225*, 129175.
[21] Sayin, S. *Luminescence* **2021**, *36*, 1716.
[22] Harikrishnan, M.; Sadhasivam, V.; Mariyappan, M.; Murugesan, S.; Malini, N.; Siva, A. *Dyes Pigm.* **2019**, *168*, 123.
[23] Du, J.; Ge, H.; Gu, Q.; Du, H.; Fan, J.; Peng, X. *Nanoscale* **2017**, *9*, 19139.
[24] Mohandoss, S.; Sivakamavalli, J.; Vaseeharan, B.; Stalin, T. *Sens. Actuators*, *B* **2016**, *234*, 300.
[25] Wang, T. T.; Liu, J. Y.; An, J. D.; Shi, Y. F.; Zhang, Y. Y.; Huo, J. Z.; Huang, Z. G.; Liu, Y. Y.; Ding, B. *Spectrochim. Acta*, *Part A* **2021**, *254*, 119655.
[26] Xia, W.; Fan, J.; Zhang, L.; Wang, J.; Du, J.; Peng, X. *J. Photochem. Photobiol.*, *A* **2018**, *355*, 165.
[27] Zhang, Y.; Zhang, L. *J. Hazard. Mater.* **2021**, *418*, 126271.
[28] Gogoi, C.; Reinsch, H.; Biswas, S. *CrystEngComm* **2019**, *21*, 6252.
[29] Ravichandiran, P.; Prabakaran, D. S.; Maroli, N.; Kim, A. R.; Park, B. H.; Han, M. K.; Ramesh, T.; Ponpandian, S.; Yoo, D. J. *J. Hazard. Mater.* **2021**, *419*, 126409.
[30] Gogoi, C.; Biswas, S. *Cryst. Growth Des.* **2021**, *21*, 2680.
[31] Yin, J. C.; Li, N.; Qian, B. B.; Yu, M. H.; Chang, Z.; Bu, X. H. *J. Coord. Chem.* **2020**, *73*, 2718.
[32] Zou, J. Y.; Li, L.; You, S. Y.; Zhang, S. W. *Inorg. Chim. Acta* **2019**, *498*, 119126.
[33] Xu, H.; Pan, Z.-R. *Chin. J. Struct. Chem.* **2019**, *38*, 2121.
[34] Zhu, H.; Li, Y. H.; Xiao, Q. Q.; Cui, G. H. *Polyhedron* **2020**, *187*, 114648.
[35] Akram, M. A.; Ye, J.; Wang, G.; Shi, L.; Liu, Z.; Lu, H.; Zhang, S.; Ning, G. *Polyhedron* **2020**, *185*, 114604.
[36] Cao, C. S.; Hu, H. C.; Xu, H.; Qiao, W. Z.; Zhao, B. *CrystEngComm* **2016**, *18*, 4445.
[37] Bai, H.; Tu, Z.; Liu, Y.; Tai, Q.; Guo, Z.; Liu, S. *J. Hazard. Mater.* **2020**, *386*, 121654.
[38] Liu, Y.; Feng, F.; Lv, G. X.; Gao, Z. S. *J. Fluoresc.* **2020**, *30*, 793.
[39] Hashemi, N.; Mousazadeh, M. H. *Opt. Mater.* **2021**, *121*, 111515.
[40] Wu, Y.; Liu, D.; Lin, M.; Qian, J. *RSC Adv.* **2020**, *10*, 6022.
[41] Qian, X.; Deng, S.; Chen, X.; Gao, Q.; Hou, Y.-L.; Wang, A.; Chen, L. *Chin. Chem. Lett.* **2020**, *31*, 2211.
[42] Ruan, B.; Yang, J.; Zhang, Y. J.; Ma, N.; Shi, D.; Jiang, T.; Tsai, F. C. *Talanta* **2020**, *218*, 121207.
[43] Wang, K.; Chen, J.; Li, H.; Zhang, M.; Liao, Q.; Wang, L.; Zhang, Y.; Niu, X. *Ionics* **2021**, *27*, 4907.
[44] Yang, Y. J.; Liu, D.; Li, Y. H.; Cui, G. H. *J. Solid State Chem.* **2019**, *278*, 120891.
[45] Guo, T. T.; Liu, Y. Y.; Yang, J.; Ma, J. F. *Inorg. Chem. Commun.* **2020**, *114*, 107847.
[46] Fu, H. R.; Zhao, Y.; Xie, T.; Han, M. L.; Ma, L. F.; Zang, S. Q. *J. Mater. Chem. C* **2018**, *6*, 6440.
[47] Gao, L.; Jiao, C.; Chai, H.; Ren, Y.; Zhang, G.; Yu, H.; Tang, L. *J. Solid State Chem.* **2020**, *284*, 121199.
[48] Jana, A. K.; Natarajan, S. *ChemPlusChem* **2017**, *82*, 1153.
[49] Zhang, Z.; Lv, T.; Tao, B.; Wen, Z.; Xu, Y.; Li, H.; Liu, F.; Sun, S. *Bioorg. Med. Chem.* **2020**, *28*, 115280.
[50] Xie, Z.; Yin, B.; Shen, J.; Hong, D.; Zhu, L.; Ge, J.; Zhu, Q. *Org. Biomol. Chem.* **2018**, *16*, 4628.
[51] Graziotto, M. E.; Adair, L. D.; Kaur, A.; Vérité, P.; Ball, S. R.; Sunde, M.; New, E. J. *RSC Chem. Biol.* **2021**, *2*, 1491.
[52] Liu, W. D.; Zhang, J.; Yin, X.; He, X.; Wang, X.; Wei, Y. *Mater. Chem. Phys.* **2021**, *266*, 124540.
[53] Shiravand, G.; Ghasemi, J. B.; Badiei, A.; Ziarani, G. M. *J. Photochem. Photobiol.*, *A* **2020**, *389*, 112261.
[54] Georgiev, N. I.; Krasteva, P. V.; Bojinov, V. B. *J. Lumin*. **2019**, *212*, 271.
[55] Zhao, Y.; Chen, K.; Yildiz, E. A.; Li, S.; Hou, Y.; Zhang, X.; Wang, Z. J.; Zhao, J. Z.; Barbon, A.; Wu, H. *Chem.-Eur. J.* **2020**, *26*, 3591.

(Zhao, C.)

